Simple Models of the Role of Surface Fluxes in Convective Cold Pool Evolution

A. N. ROSS

Institute for Atmospheric Science, School of the Environment, University of Leeds, Leeds, United Kingdom

A. M. TOMPKINS

ECMWF, Reading, United Kingdom

D. J. PARKER

Institute for Atmospheric Science, School of the Environment, University of Leeds, Leeds, United Kingdom

(Manuscript received 16 June 2003, in final form 4 January 2004)

ABSTRACT

Gravity-current models have been used for many years to describe the cold pools of low-level air that are generated by cumulonimbus precipitation. More recently, it has been realized that surface fluxes of heat and water vapor can be important in modifying these flows, through turbulent mixing of buoyancy by convection, and through direct modification of the cold pool buoyancy. In this paper, simple models describing the role of surface fluxes in depleting the negative buoyancy of a gravity current and the consequences of this for the flow dynamics are discussed.

It is pointed out that the depletion of cold pool buoyancy by surface fluxes is analogous to the depletion of buoyancy in a turbidity current through particle sedimentation, and in one regime of parameter values the analogy is exact. This analogy allows one to use simple flow models that have been tested extensively against laboratory experiments on turbidity currents. A simple ''box model'' and a more sophisticated shallow water model are each developed. It is shown how these models can give relatively simple expressions for cold pool ''runout length'' and buoyancy distributions. These runout lengths compare well with maximum cold pool sizes previously observed in cloud-resolving model simulations of unorganized tropical deep convection.

1. Introduction

In the Tropics, deep convection and the large-scale dynamical circulation are intimately tied, and thus it is important to gain an appreciation of the factors that control the organization and temporal variability of the former. In addition to feedbacks with radiation (e.g., Slingo and Slingo 1988), water vapor (Tompkins 2001a,c; Grabowski 2003), and large-scale atmospheric waves (Emanuel et al. 1994), it has also been suggested that cold pools, formed from the negatively buoyant downdraft air, could play a role in convective organization. This role has mostly been regarded as a dynamical one, where environmental boundary layer air is forced over the spreading cold pool outflow, and is thereby mechanically lifted through the negatively buoyant layer to reach the level of free convection (LFC) and thus initiate a new convective cell (e.g., Simpson 1980).

Corresponding author address: Dr. A. N. Ross, Institute for Atmospheric Science, School of the Environment, University of Leeds, Leeds, LS2 9JT, United Kingdom.
E-mail: aross@env.leeds.ac.uk

In order to investigate this and other characteristics of convective cold pools, they have usually been regarded as a density current, a flow where a fluid of one density flows into a fluid of a different density as a result of the horizontal density difference. This concept has been widely applied to atmospheric (such as mesofronts and sea breezes) and other geophysical flows (e.g., oceanic turbidity currents and freshwater intrusions in fjords and estuaries). Simpson (1997) provides an extensive overview of the many applications.

Much of the theoretical and experimental work on density currents has concentrated on idealized problems, often with channel flow or axisymmetric releases of fluid. These generic examples can then be applied in many different fields.

The simplest case is where the density of the two fluids remains constant with no loss of buoyancy. In the laboratory this is commonly achieved using saline solutions and freshwater. Extensive studies have been carried out with both channel and axisymmetric currents, for example, Simpson and Britter (1980) and Huppert and Simpson (1980). In these studies the current is shown to be divided into two main regions. Near the

front of the current is the head region, which is characterized by deeper and relatively dense fluid. Behind the head is a much shallower region of fluid. Measurements of the head size and speed show that the motion of the density current is predominantly governed by the head. In circumstances where the depth of the layer of light fluid is much greater than the depth of the head then the relationship

$$\mathrm{Fr} = u/(g'h)^{1/2} \tag{1}$$

is observed where Fr, the Froude number, is a constant with an experimental value of around 1.2 (see Huppert and Simpson 1980). The same relationship was found theoretically for an inviscid, immiscible current in a channel by Benjamin (1968), although the constant in that case was slightly larger with a value of $\sqrt{2}$. Theoretical models for density currents, for example the integral model of Huppert and Simpson (1980) or the shallow water model of Hoult (1972), often make use of this ''Froude number condition'' on the front. Integral models are the simplest form of theoretical model, assuming the entire current has a uniform height and remains well mixed. Such models, despite their simplicity, often perform surprisingly well in comparison with laboratory studies (e.g., Huppert and Simpson 1980).

The next level of sophistication in models of density currents is those based on the shallow water equations. These allow variations in height along the current and can capture the distinction between the head and tail regions of the flow. For both channel and axisymmetric flows with an instantaneous release of dense fluid there are similarity solutions to these equations (see, e.g., Hoult 1972; Grundy and Rottman 1985). These solutions indicate the long-time behavior of the flow once the effects of the initial conditions have become unimportant. These similarity solutions are in good agreement with both laboratory experiments and atmospheric measurements of phenomena such as sea breezes (e.g., Rottman and Simpson 1983).

Despite the documentation of cold pool–enhanced surface fluxes, most previous numerical investigations have neglected their effect on the cold pool evolution. Often, cold pools are initiated from a constant temperature source, and the evolution of a single density current cold pool is investigated, in which the water vapor field plays no role (Moncrieff and Liu 1999; Liu and Moncrieff 2000; Parker 1996). This approach was adopted since the focus of these studies was dynamical: investigating the control of the cold pool by the mean flow, neglecting surface fluxes. They examined the turbulent dynamics of the wake head, or the dynamical triggering of new convection when ambient boundary layer air is forcibly lifted over the spreading cold pool (e.g., Droegemeier and Wilhelmson 1987). Much has been learned from such studies, which have documented this triggering mechanism for a variety of vigorous convective systems, such as squall lines or the collision of sea-breeze fronts (Kingsmill 1995).

There have been few studies of the effect of surface fluxes on cold pools. Linden and Simpson (1986) carried out idealized laboratory experiments on the effect of turbulent convection on a gravity current by passing bubbles through a saline gravity current. With sufficient turbulence (sufficiently high heat fluxes) the head structure of the gravity current was broken down to give a vertically well mixed structure to the flow and a gentle horizontal density gradient. Once the turbulence was removed the gravity current quickly reformed. Similar effects were observed in the atmosphere by Reible et al. (1993) who showed the strengthening of sea-breeze fronts in the evening with the decay of convective turbulence. Over the ocean convective turbulence is much weaker than over land and is generally not sufficient to lead to this type of disruption of the gravity current.

A recent investigation of tropical deep convection used a different approach to investigate the role of cold pools. Tompkins (2001b) operated a cloud-resolving model with a 350-m horizontal resolution to an equilibrium state, and documented the evolution of the cold pools by conditional sampling, similar to observational data analysis techniques (e.g., Young et al. 1995). In this way the cold pool evolution is as realistic as possible, especially regarding the role of the water vapor, bearing in mind the limitations imposed by our knowledge (parameterization) of pertinent processes involved and by the resolution. The study came to the unexpected conclusion that in cases of low wind shear where deep convection is apparently ''unorganized,'' the cold pools still played a crucial role in the triggering of new convective events, and therefore also the degree of clustering of the convection. However, rather than the dynamical lifting mechanism previously assumed, the study found that the triggering procedure was strictly thermodynamical. Boundary layer air in the root region of convection was observed to have higher initial equivalent potential temperature (θ_e), as seen in observations (Kingsmill and Houze 1999). This air is ''preconditioned'' by the evaporation of rainfall, which introduces negative buoyancy and positive humidity anomalies. This negatively buoyant air is pushed out by the subsequently developing cold pool. Surface fluxes of water vapor sustain the humidity anomaly, opposing the action of mixing at the wake head, while sensible heat fluxes aid the recovery of the negative buoyancy anomaly. Once the buoyancy anomaly is removed, it is this high θ_e air on the boundary of the convective wake that spawns a new convective cell. In this view, it is thus the surface fluxes that largely determine the radius at which new cells are triggered.

Although Tompkins (2001b) was able to provide a number of examples in the literature where several of these cold pool features are observed, such as the higher initial boundary layer θ_e, the thermodynamic role of rainfall evaporation before the onset of the cold pool, and the double front structure of convective wakes (where the dry humidity anomaly occurs behind the gust

front), the study left a number of issues unanswered. The thermodynamical and dynamical evolution of cold pools involves a number of concurrent processes, and the relative roles of the evaporation of rainfall and entrainment with respect to the surface fluxes is unclear, and difficult to determine from such a complex model. Therefore, the evolution of cold pools is further investigated here using a series of simpler models, in which the isolation of individual physical processes is facilitated. The aim of this paper is to demonstrate the usefulness of simple models of density-current dynamics in describing cold pool evolution in conditions of surface heating. Such models may be applicable to the development of convective parameterization schemes.

2. Mechanisms for buoyancy reduction in a density current

It has been found that constant buoyancy is an adequate assumption in many cases of gravity currents where external sources of buoyancy are small. However, there are several applications where buoyancy sources, such as surface heating, can play an important role.

One obvious cause of changes in buoyancy or density in a density current is the entrainment of ambient fluid into the current or detrainment of fluid into the ambient. Two mechanisms for this mixing can be envisaged. The first is the instability of the density and velocity interface between the density current and the ambient. The instability leads to the formation of Kelvin–Helmholtz-like billows on the interface, which can detrain fluid from the current and mix in ambient fluid. This generally leads to the formation of a mixed layer of fluid behind the head and above the thin tail region of the current. This mixed layer generally has a neutral Richardson number and inhibits further entrainment into the tail. The second mechanism operates when the density current is traveling along a rigid surface; the no-slip boundary condition results in a thin layer of ambient fluid being overrun by the advancing density current head. This is statically unstable and results in the lighter ambient fluid rising up through the head forming the characteristic ''lobe and clef'' structure of a density current head.

Several laboratory studies (e.g., Hacker et al. 1996; Hallworth et al. 1996) have attempted to measure the entrainment into density currents. Comparison by Hallworth et al. (1996) of free-surface (free slip) and rigid surface (no slip) density currents suggests that the overrunning fluid mechanism accounts for approximately two-thirds of the entrainment into a density current head. The results also suggest that the entrainment into the head is minimal during the slumping phase of the flow. The slumping phase is the initial period after the release of a gravity current in which it adjusts toward the classical gravity current shape shown in Fig. 1 (see, e.g., Huppert and Simpson 1980). The traditional model for the structure of a density current involves the fluid in the tail region of the flow traveling faster than the head. As fluid is detrained from the rear of the head by billows on the interface it is replaced by dense fluid from the thin tail region, thus ensuring that the density of the head changes only slowly. Initially this fluid being carried into the head from behind has a density comparable to the release density, but in the later stages of the flow it becomes diluted by mixing across the interface of the tail with the ambient. This leads to a gradual decrease in the density of fluid in the head. More recent work has suggested that this view of fluid from behind entering the head may in fact not be correct. Lowe et al. (2002) have made careful measurements of the velocity structure within an intrusive density current, which suggest that the fluid from the tail that is moving forward relative to the head is in fact washed out of the current by the billows before reaching the head. This means the head of the current is not significantly affected by the detrainment of fluid by the billows and retains its density significantly longer than might be expected. Of course, for a density current on a rigid surface, the overrunning mechanism will still entrain ambient fluid into the head.

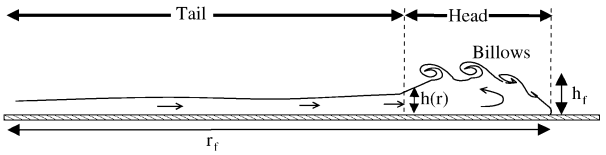

FIG. 1. Schematic diagram illustrating the structure of a gravity current. The distinction between the relatively deep head region and the shallower tail region behind is shown. The interface between the head and the ambient fluid is characterized by billows caused by a shear instability on the interface. The arrows inside the gravity current give an indication of the assumed circulation within the current.

Another commonly studied example of varying buoyancy is the particle-driven density current, for example, turbidity currents in the laboratory or ocean. In these density currents, the density difference is a result of the particles suspended in the fluid increasing the bulk density. Over time these particles settle out under gravity, reducing the density difference that is driving the flow. These flows can be studied relatively easily in the laboratory (see, e.g., Bonnecaze et al. 1993, 1995). Theoretical approaches based on integral models and the shallow water equations have been extended to these particle driven flows assuming the particles only leave the flow through the viscous sublayer near the lower surface and remain well mixed throughout the rest of the flow. These models generally agree well with the experimental data for moderate-sized particles provided the particle concentrations are not very high or very low. Huppert (1998) provides a good review of the various approaches to modeling these flows and a discussion of some of the applications.

The problem of a particle-driven density current can be extended by supposing the interstitial fluid in the current is lighter than the ambient fluid. This can lead to interesting behavior when the current is initially dens-

er than the ambient and so travels as a density current. After sufficient particles have settled out the current will become lighter than the ambient and will ''lift off.'' Laboratory experiments of this phenomena and comparisons with integral and shallow water models have been conducted by Hogg et al. (1999). The lift-off distance can be predicted with a fair degree of accuracy using a simple integral model, although this tends to underpredict the distance for interstitial fluids with densities close to the ambient, while it overpredicts for very light interstitial fluids.

Evolution of the buoyancy in a density current could also result from a thermodynamic contrast with the surface below, resulting in heating. In contrast to the above examples, there has been little study of density currents that are modified by latent and/or sensible heat fluxes during their evolution. Those studies that have taken place (Linden and Simpson 1986) have concentrated on the effect of the heat flux in promoting turbulent convection rather than the role the sensible heat flux plays in altering the buoyancy. The convectively generated cold pool is an example of such a flow, since the underlying surface is generally warmer and moister than the cold pool. Indeed, the increased wind speeds, and large perturbations to the temperature and moisture fields result in a significant amplification of the surface fluxes of sensible and latent heat, in some cases more than doubling the ambient values (e.g., Jabouille et al. 1996). Some simple models, for example, Raymond and Zeng (2000) and Qian et al. (1998), have used this mechanism in the parameterization of deep convection.

Tompkins (2001b) has proposed that the surface fluxes into a cold pool can play an important role in the triggering of deep convection. The mechanism also requires the persistence of a band of high humidity and θ_e near the front of the current. If detrainment of the moist air from this region were rapid compared to the time over which the surfaces fluxes warm the current, then the mechanism would not be relevant to the atmosphere. Although a detailed understanding of the entrainment in the head is still not possible there is evidence both from cloud-resolving model (CRM) results and from laboratory experiments that the humid region does persist. In the following sections we shall assume that this is the case and ignore the role of entrainment. The relevance of this will be discussed further in section 7.

3. A shallow water model

a. Model description

It has been suggested by Tompkins (2001b) that it is the water vapor on the outer edges of the downdraft outflow that controls the triggering of convection. The spacing of the convective activity is therefore controlled by the extent of the cold pool regions. The cold pool can be considered as a density current (e.g., Goff 1976; Simpson 1980). The propagation of the current depends on the effective (or reduced) gravity

$$g' = g\frac{\theta_{v0} - \theta_v}{\theta_{v0}}, \tag{2}$$

where θ_v is the virtual potential temperature. This is positive for a cold pool.

In general, the cold pools formed by tropical convection may be a few hundred meters deep, but extend up to 20 km in radius. This means the horizontal scale of the motion tends to be much larger than the vertical scale (except possibly near the front of the pool and near the downdraft) so the shallow water equations are a suitable means of modeling this type of flow. Since we are considering flow in low wind shear, we shall assume the cold pool remains axisymmetric. The pool can then be described by the equations

$$\frac{\partial h}{\partial t} + \frac{1}{r}\frac{\partial}{\partial r}(ruh) = 0, \quad \text{and} \tag{3}$$

$$\frac{\partial}{\partial t}(uh) + \frac{1}{r}\frac{\partial}{\partial r}(ru^2h) + \frac{1}{2}\frac{\partial}{\partial r}(g'h^2) = 0, \tag{4}$$

where $h(r, t)$ is the depth and $u(r, t)$ is the radial velocity of the density current.

As mentioned, the shallow water equations are not valid at the front of the density current. Some further condition is needed to close the problem. The most common is the constant Froude number condition (1).

One important difference between real cold pools and much of the previous theoretical work on density currents is the role that the thermodynamics plays in altering the effective gravity, and hence the driving force behind the current. We shall assume that the warming of the cold pool is principally due to surface heat fluxes, as discussed in section 2. We shall neglect the effects of entrainment. Away from the source of the cold pool; evaporation of precipitation is not relevant and will also be ignored.

Heat fluxes are calculated assuming a simple bulk aerodynamic formula, giving the virtual potential temperature as

$$\frac{\partial \theta_v}{\partial t} + u\frac{\partial \theta_v}{\partial r} = \frac{C_d}{h}(u + u_0)(\theta_{vs} - \theta_v), \tag{5}$$

where C_d is the dimensionless drag coefficient and θ_{vs} is the imposed surface virtual potential temperature (assumed constant).

In the surface flux calculation the cold pool radial velocity is enhanced by a constant wind u_0, which can be interpreted in two ways. If the deep convective event were occurring in a motionless background state, u_0 would represent the bulk flux formula correction for low wind conditions. Beljaars (1995) indicates that a reasonable value for u_0 is around 1 m s^{-1} over oceans,

although a higher value may be appropriate over land.[1] Thus, in this case it is reasonable to assume $u_0 \ll u$, and u_0 can be reasonably neglected in a simple model. An alternative scenario is that the cold pool occurs in a situation of mean background wind, with zero or very limited vertical wind shear throughout the boundary layer. In such a steady laminar flow, the wind shear will be restricted to a narrow layer near the surface and is unlikely to interact significantly with the turbulent head dynamics, such as investigated by Parker (1996), Moncrieff and Liu (1999), and Liu and Moncrieff (2000). In this case, the cold pool is advected by the mean flow, and (5) approximately describes the evolution of the cold pool in a Lagrangian framework in the downwind direction in which the cold pool winds enhance surface fluxes. If a background wind exceeding roughly 5 m s^{-1} is chosen, then a simple model can reasonably make the other extreme assumption in this case that $u \ll u_0$. By substituting in Eq. (2), one can show that Eq. (5) still holds with g' and g'_s replacing θ_v and θ_{vs}.

b. Analogy with particle-laden density currents

Provided the cold pool velocity is relatively slow compared to u_0, which will certainly be true for the later stages of the flow, a reasonable first approximation is to neglect the contribution of the cold pool velocity to the heating, and hence

$$\frac{\partial g'}{\partial t} + u\frac{\partial g'}{\partial r} = \frac{C_d u_0}{h}(g'_s - g'). \tag{6}$$

It is interesting to note that the system of Eqs. (3), (4), and (6) is now equivalent to the shallow water equations for a particle-driven density current given by Bonnecaze et al. (1995) with the role of the particle settling velocity v_s being taken by the aerodynamic drag term $C_d u_0$. The effect of an interstitial fluid in the current that is lighter than the ambient fluid is replaced by the imposed temperature difference between the ambient and the surface, represented through g'_s.

Unlike the thermal cold pool problem, these particulate flows are easily modeled in the laboratory and have been extensively investigated. Bonnecaze et al. (1995) provide numerical solutions to the shallow water equations with $g'_s = 0$ and compare these with laboratory experiments. For a constant volume release the agreement between experiment and theory is very good. The front position of the current is well predicted, although there is some discrepancy in the pattern of deposited particles. While there is some evidence that particles are swept along the floor in the experiments, the discrepancy is also partly related to the prediction of a strong bore near the source, which is not observed in the experiments. While Bonnecaze et al. (1995) are unable to offer a clear explanation of this, it is presumably a limitation in the shallow water model. This limitation does not appear to seriously impair the ability of the model to predict the propagation and development of the front, and so the shallow water model may still be a useful predictive tool.

By suitably nondimensionalizing the shallow water equations the dependence on v_s can be removed so it only appears in the initial conditions. Provided the current travels a sufficient distance that $r \gg r_0$ (where r_0 is the initial cold pool radius) then the maximum runout length should be independent of the initial conditions and merely proportional to the nondimensional length $(g'V^3/v_s^2)^{1/8}$. The coefficient depends on the exact definition of the runout length. Taking the runout length as the front position at the time when g' has reduced to 0.1% of its initial value, Bonnecaze et al. (1995) give the coefficient of proportionality as 1.9. We shall use this definition of the runout length.

The case with a light interstitial fluid (corresponding to a surface warmer than the ambient) is studied by Hogg et al. (1999), although they only consider the two-dimensional channel problem. In this case the current "lifts off" when sufficient particles have settled out that the bulk density of the current is less than the ambient. The point at which this occurs depends on the relative densities and initial concentrations of the particles and the interstitial fluid, with the distance becoming smaller as the interstitial fluid becomes less dense. This provides a graphical example of the potential of a density current to trigger convection. In the next section this will be examined numerically in the context of convective cold pools.

4. Numerical solutions of the shallow water model

a. Model description and validation

Full numerical solutions of the shallow water equations (3), (4), and (6) can be obtained and compared with the above asymptotic expansions. The equations are first transformed using the substitution $y = r/r_N$ so that the current always occupies the region $0 \le y \le 1$. The equations are solved using the Simple High Accuracy Resolution Program (SHARP) flux-limiter scheme (Leonard 1988). The accuracy in time is improved by using the Richardson extrapolation (see Press et al. 1992). Since the shallow water equations permit the formation of shocks and these can occur in the solution for an axisymmetric density current, it is necessary to add an artificial viscosity term, as done by Bonnecaze et al. (1995), to ensure numerical stability.

The model has been validated against the similarity solutions of the shallow water equations in the absence of heating (not shown). After an initial adjustment period during which the initial conditions are important,

[1] This should not be confused with the larger (roughly, 5 m s^{-1}) wind enhancement often applied in general circulation models (GCMs), which is dominated by the mesoscale fluctuations (e.g., Redelsperger et al. 2000; Zeng et al. 2002).

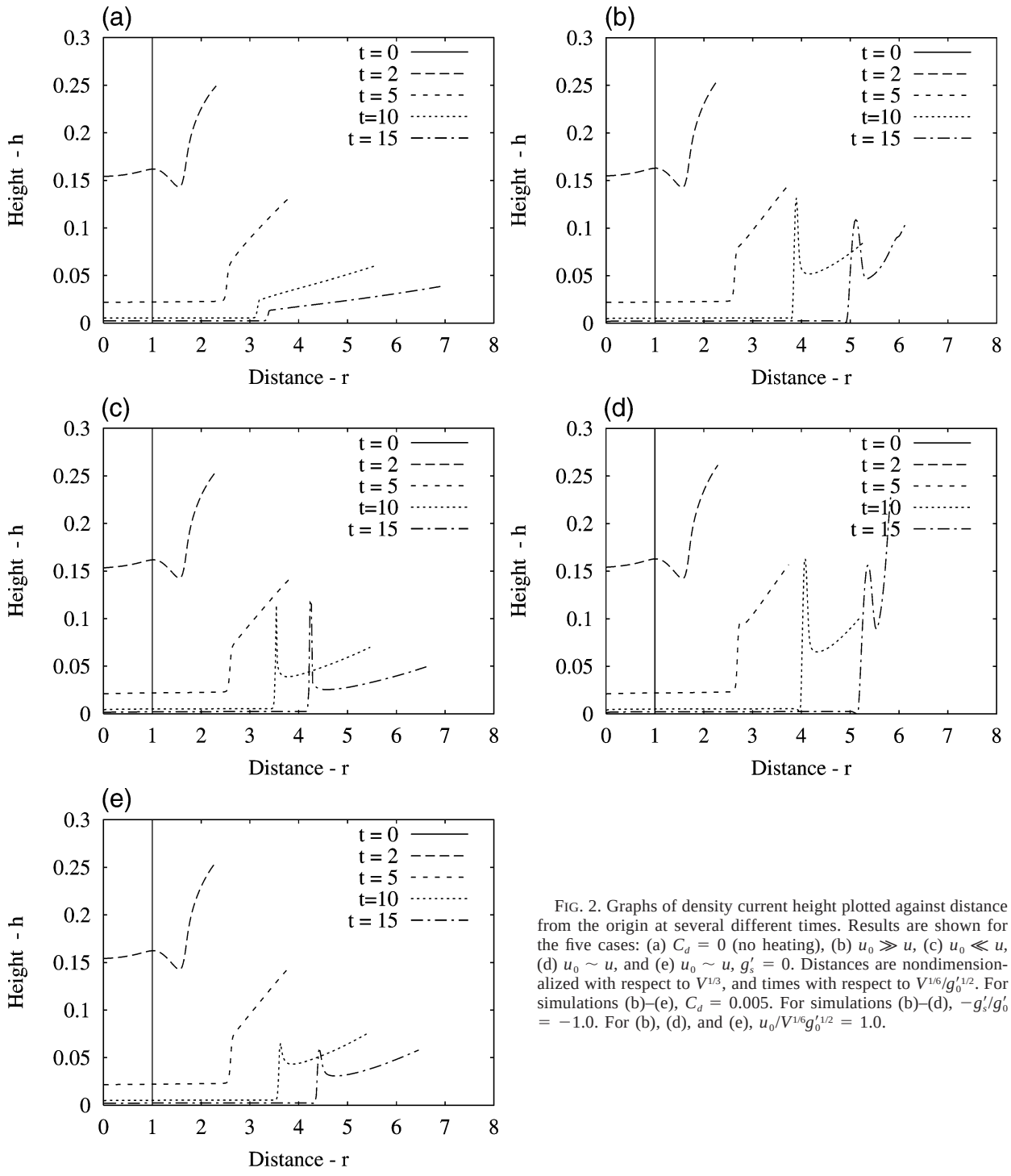

FIG. 2. Graphs of density current height plotted against distance from the origin at several different times. Results are shown for the five cases: (a) $C_d = 0$ (no heating), (b) $u_0 \gg u$, (c) $u_0 \ll u$, (d) $u_0 \sim u$, and (e) $u_0 \sim u$, $g'_s = 0$. Distances are nondimensionalized with respect to $V^{1/3}$, and times with respect to $V^{1/6}/g'^{1/2}_0$. For simulations (b)–(e), $C_d = 0.005$. For simulations (b)–(d), $-g'_s/g'_0 = -1.0$. For (b), (d), and (e), $u_0/V^{1/6}g'^{1/2}_0 = 1.0$.

the numerical solution converges to the similarity solution for a large range of times.

Figures 2–4 show cross sections of the height, effective gravity, and radial speed of a developing density current with various different types of heating. The figures marked (a) are in the absence of any heating. In this case the current rapidly forms into a relatively deep head with a shallower region behind (Fig. 2a). As expected, in the absence of heating, Fig. 3a shows that g' remains constant. The maximum speed in the current (Fig. 4a) corresponds to the back of the head region where there is a rapid change in height. This is not in exact agreement with the shallow water similarity solution, which predicts that, at a given time, u will in-

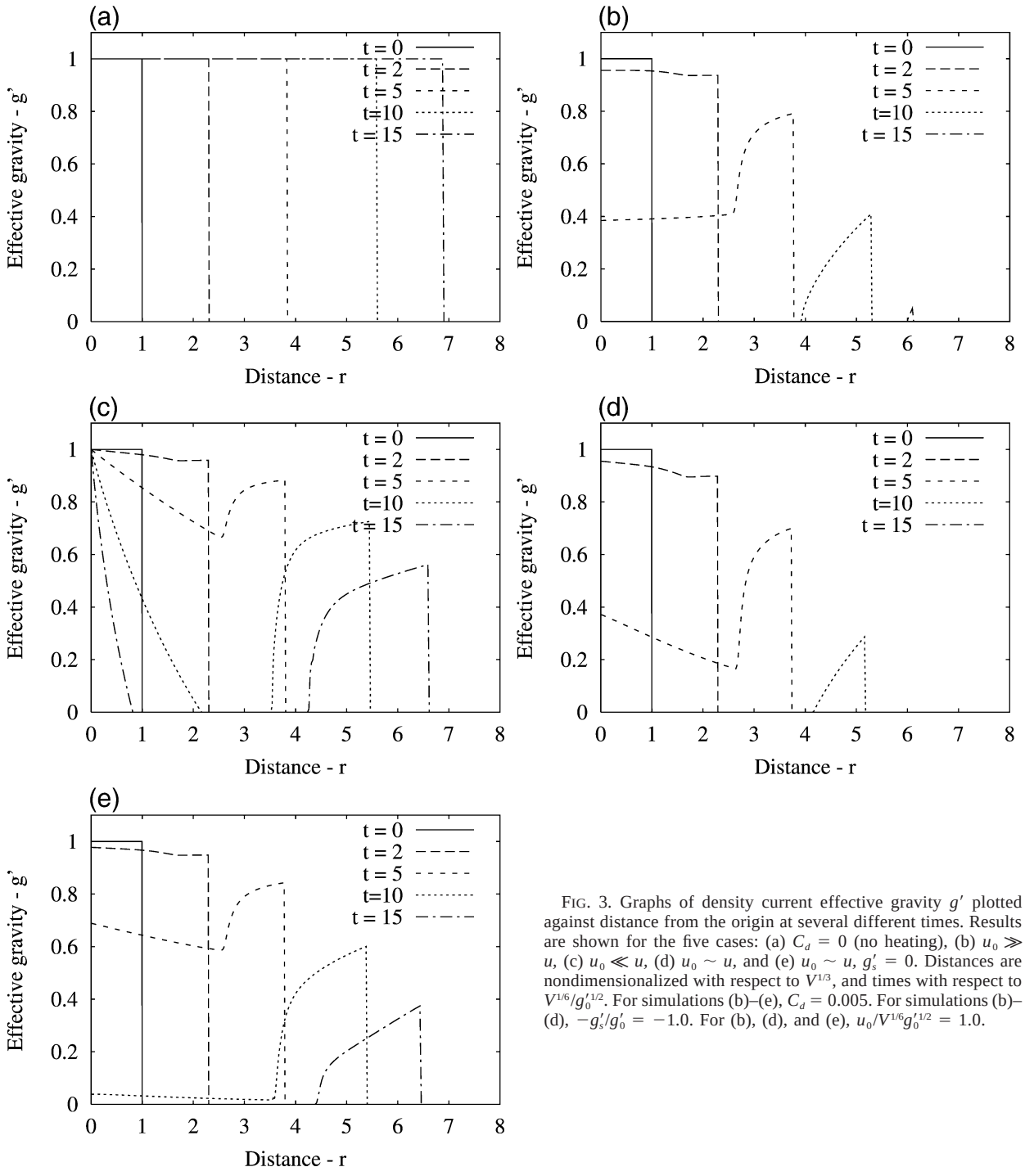

FIG. 3. Graphs of density current effective gravity g' plotted against distance from the origin at several different times. Results are shown for the five cases: (a) $C_d = 0$ (no heating), (b) $u_0 \gg u$, (c) $u_0 \ll u$, (d) $u_0 \sim u$, and (e) $u_0 \sim u$, $g_s' = 0$. Distances are nondimensionalized with respect to $V^{1/3}$, and times with respect to $V^{1/6}/g_0'^{1/2}$. For simulations (b)–(e), $C_d = 0.005$. For simulations (b)–(d), $-g_s'/g_0' = -1.0$. For (b), (d), and (e), $u_0/V^{1/6}g_0'^{1/2} = 1.0$.

crease linearly with r. However, such shocks are observed in other numerical studies, such as those of Grundy and Rottman (1985) and Bonnecaze et al. (1995), and also in laboratory experiments where the density current is observed to form a deep head region with a much shallower tail region. This is particularly noticeable with axisymmetric currents where the geometric stretching of vortex lines in the head tends to strengthen the head region. Experimental measurements of fluid speed in two-dimensional density currents by Britter and Simpson (1978) give the speed of flow into the head as approximately 22% greater than the speed of the front, again showing deviation from the similarity solution.

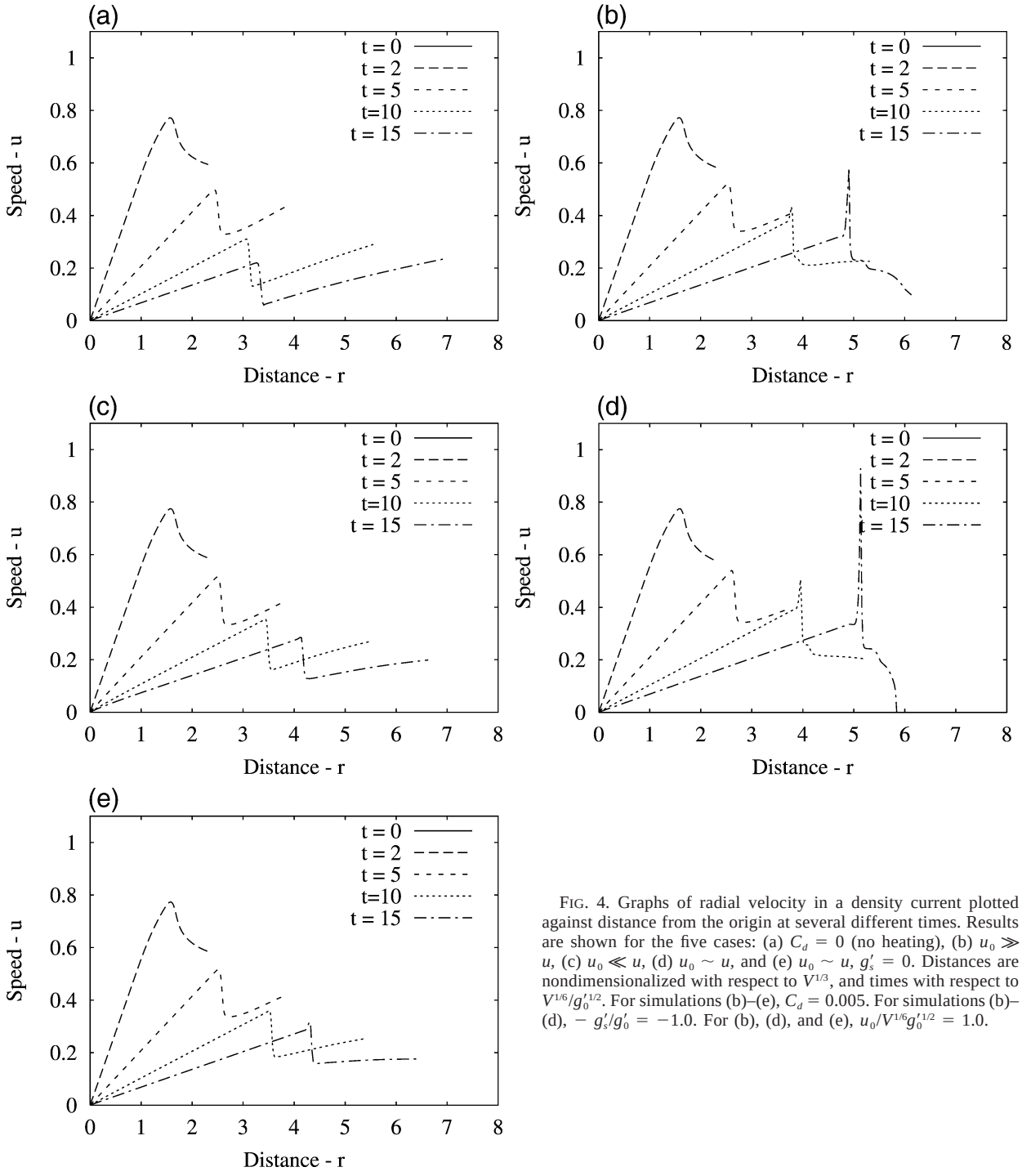

FIG. 4. Graphs of radial velocity in a density current plotted against distance from the origin at several different times. Results are shown for the five cases: (a) $C_d = 0$ (no heating), (b) $u_0 \gg u$, (c) $u_0 \ll u$, (d) $u_0 \sim u$, and (e) $u_0 \sim u$, $g_s' = 0$. Distances are nondimensionalized with respect to $V^{1/3}$, and times with respect to $V^{1/6}/g_0'^{1/2}$. For simulations (b)–(e), $C_d = 0.005$. For simulations (b)–(d), $-g_s'/g_0' = -1.0$. For (b), (d), and (e), $u_0/V^{1/6}g_0'^{1/2} = 1.0$.

A further test of the numerical model was undertaken by comparing the numerical predictions (not shown) with those presented by Bonnecaze et al. (1995) for a particulate density current with nondimensional settling velocity $\beta = 0.005$ and no interstitial fluid. The model was able to reproduce the graphs of height, velocity, and concentration given in Bonnecaze et al. (1995).

b. Shallow water predictions with heating

The shallow water model is used to investigate the range of assumptions concerning the cold pool heating outlined in section 3, neglecting in turn the background wind u_0 and the cold pool perturbation wind u, and finally considering the full solution including both com-

ponents. All results are presented in a nondimensional form and here we assume an arbitrary nondimensional value of 1 for u_0 as an illustrative case. Similar solutions may of course be trivially obtained for different values of u_0. Figures 2b, 3b, and 4b correspond to the case $u_0 \gg u$, which is analogous to the problem of a particle-laden density current with an interstitial fluid lighter than the ambient fluid. The current is seen to propagate more slowly as a result of the surface heating. This means that the current is actually deeper than the corresponding current without heating and that the shock at the back of the head is stronger. Initially the current heats up reasonably uniformly, but as the distinction between the head and the tail becomes more distinct, the tail warms much more rapidly as it is much shallower. Within the head region, the temperature increases (corresponding to a decrease in g') from the front of the head to the rear of the head. Although there appears to be a shock and numerical overshoot in the predicted height at the rear of the head, the temperature in this region is almost equal to the ambient temperature, so this has little influence on the dynamics of the current. Plots of the buoyancy $g'h$ (not shown) are smooth and show no sign of the instability. The overshoot in the current height at the rear of the head is observed in the majority of cases with heating, but in all these cases it does not appear in the buoyancy. At early times the speed profile along the current does not vary significantly from the case without heating (see Fig. 4). As the current develops, however, the speed in most of the head can actually increase, although there is a tendency for the speed to decrease toward the front of the head, unlike the case without heating where the speed increases toward the front. The front speed is lower in the case with heating as the heating reduces the temperature difference between the density current and the ambient, and it is this temperature difference that drives the current forward via the front Froude number condition.

To assess the impact of the overshoot at the rear of the head case (b) was rerun with a higher-resolution grid. The results showed that with an increased resolution the shock was better resolved. There was also an increase in the height of the overshoot. Away from the shock the differences in the current height and speed were negligible between different resolution runs. In particular, increasing the resolution made no difference to the front position or density, which are of particular interest in this paper. This can be partly explained by realising that it is the buoyancy $g'h$ that is important in driving the flow and not h itself. There is no evidence of overshoot in profiles of $g'h$ since g' is zero in regions where the overshoot in the height and speed occur.

The complementary case where $u_0 \ll u$, that is, u_0 is negligible, is shown by the figures labeled (c). In this case the differences between the case without heating are much less. This is principally due to the the fact that although initially $u \sim 1$, it rapidly decreases so the total heating is much less than in case (b) where u_0 was fixed at 1.0. Apart from an increase in the overshoot at the rear of the head, the height profiles are very similar between cases (a) and (c). The speed profiles are also similar, although the front speed in case (c) is slightly lower. Figure 4c also shows that the head is slightly smaller in the case with heating. The principal difference lies in the profiles of effective gravity. The heating is greatest at the front of the tail region, just behind the head, where the speeds are largest and the flow is shallow. The temperature in this region rapidly approaches the ambient value. Near the origin temperatures remain lower since the flow speed is low and less heating occurs. The temperature increases from the front to the back of the head region, although the dropoff at the back of the head is much more rapid than in case (b). This is related to the more constant head height in case (c).

Case (d) shows the combined effect of both the u and u_0 terms on the heating. Results are very similar to case (b). As mentioned above, although u is initially about 1.0 in this case, it rapidly falls so that the u_0 term dominates the cooling after the initial stages. The heating is slightly greater than in case (b) and this is reflected in the slightly reduced front speed and the slightly smaller size of the head at a given time.

For cases (b)–(d) the surface temperature was higher than the ambient temperature so the surface heating will remain important even as the density current approaches the ambient temperature. Case (e) includes the effects of both u and u_0 on the heating, but has the surface temperature equal to the ambient temperature. This results in much reduced surface heating rates. In many ways the results are similar to case (c), which also had a smaller heating rate since u rapidly became much less than 1.0. The primary difference is that the temperature near the origin rapidly increases toward the ambient in this case because of the action of the u_0 term.

Figure 5 shows the front position of the density current against time for each of the cases (a)–(e). It can be seen that, at least at early times, the presence of heating makes only a moderate difference to the propagation of the density current. Once the heating has significantly altered the temperature of the cold pool, then the propagation of the current is reduced and eventually the current is dissipated. In general terms, it is the amount of heating that determines how long the current takes to dissipate and its maximum extent.

5. Integral models of a cold pool

a. An integral model

As discussed above, integral models are often in surprisingly good agreement with laboratory experiments, and have the advantage of analytical simplicity (see, e.g., Huppert and Simpson 1980). Let us assume that the current has a uniform height and is well mixed

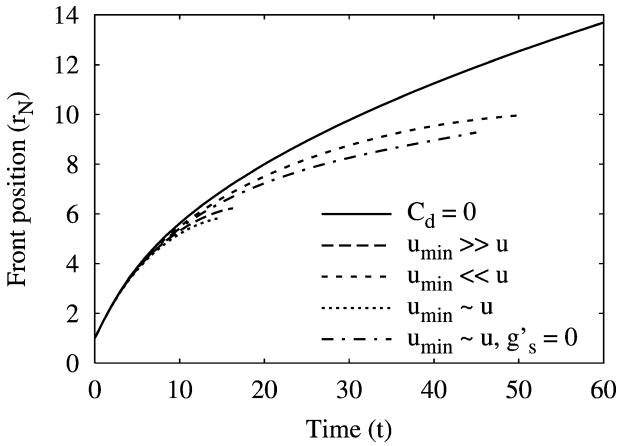

FIG. 5. Graphs of density current front position as a function of time. Results are shown both with and without the contribution of the u and u_0 terms in the surface heat fluxes. Distances are nondimensionalized with respect to $V^{1/3}$, and times with respect to $V^{1/6}/g_0'^{1/2}$. For these simulations $C_d = 0.005$, $u_0 = 1.0$, and $g_s' = -1.0$, unless otherwise stated.

throughout. Let the radius of the current be r and the height h. The volume of the current is unchanged so $V = \pi r^2 h$ is a constant. The front Froude number condition controls the speed of the current so

$$\frac{dr}{dt} = \mathrm{Fr}\sqrt{g'h}. \tag{7}$$

The density of the current is reduced through the surface heat flux so

$$\frac{dg'}{dt} = \frac{C_d}{h}(u_0 + u)(g_s' - g'). \tag{8}$$

Combining (7) and (8) gives a differential equation

$$\frac{dg'}{dr} = \frac{C_d \pi}{V} r^2 \left(\frac{u_0 \pi^{1/2}}{\mathrm{Fr} V^{1/2}} r g'^{-1/2} + 1 \right)(g_s' - g') \tag{9}$$

for g' in terms of r. In general, this requires numerical integration, but further progress can be made in the two interesting limits of $u \ll u_0$ and $u \gg u_0$.

b. A slow density current: $u \ll u_0$

In cases where the speed of the density current is much less than the minimum wind speed u_0 used to calculate the surface heat fluxes, then the effect of the current speed can be neglected.

With this simplification we can neglect the term 1 in (9) compared to the term containing u_0 and can integrate to get

$$1 - \left(\frac{g'}{g_0'}\right)^{1/2} + \alpha \tan^{-1}\left[\frac{(g'/g_0')^{1/2}}{\alpha}\right] - \alpha \tan^{-1}\left(\frac{1}{\alpha}\right) = \frac{C_d u_0 \pi^{3/2}}{8 \mathrm{Fr} g_0'^{1/2} V^{3/2}}(r^4 - r_0^4). \tag{10}$$

Recalling that $g_s' < 0$ for a warm surface, $\alpha = (-g_s'/g_0')^{1/2}$ measures the relative magnitudes of the surface temperature anomaly and the initial cold pool anomaly. The maximum extent of the density current corresponds to the location at which $g' = 0$. Substituting this in (10) gives an expression for this maximum distance r_{crit} of

$$r_{\mathrm{crit}} = \left[r_0^4 + \frac{8 \mathrm{Fr} V^{3/2} g_0'^{1/2}}{C_d u_0 \pi^{3/2}} \left(1 - \alpha \tan^{-1}\frac{1}{\alpha} \right) \right]^{1/4}. \tag{11}$$

Assuming that $r_{\mathrm{crit}} \gg r_0$ then $r_{\mathrm{crit}} \propto (\mathrm{Fr} V^{3/2} g_0'/C_d u_0)^{1/4}$, as predicted by Bonnecaze et al. (1995) for a current with $g_s' = 0$. The increased heat flux as a result of the warm surface reduces the maximum extent by a factor $[1 - \alpha \tan^{-1}(1/\alpha)]^{1/4}$.

To find the extent and potential temperature anomaly of the cold pool as a function of time requires numerical solution of (7) and (8) since g' cannot be written explicitly in terms of r using (10). In the special case where $g_s' = 0$ and so $\alpha = 0$, analytic solutions can be obtained (see Bonnecaze et al. 1995 for details).

Figure 6a shows a comparison of the runout length from numerical solutions of the shallow water model and the predictions of the integral model as a function of the parameter α that measures the relative magnitude of the surface heat anomaly and the cold pool anomaly. The first point to note is that nondimensionalizing the maximum shallow water distance by $C_d u_0 / V^{3/2} g_0'^{1/2}$ collapses the data well, showing that the dependence on the aerodynamic drag is the same as for the integral model. On the other hand, the shallow water model predicts significantly larger maximum radii for the cold pool than the integral model. The reason for this is lies in the fact that g', h, and u vary greatly along the current and are not uniform as assumed by the integral model. Bonnecaze et al. (1995) observed a similar discrepancy between shallow water and integral model solutions for the case with $\alpha = 0$, with the integral model predicting a runout length of only 60% of the shallow water value.

c. A fast density current: $u \gg u_0$

In cases where the speed of the density current is much greater than the minimum wind speed u_0, then u_0 can be neglected. This condition cannot be true everywhere since we enforce $u = 0$ as a boundary condition at the origin, but for a fast enough current, this small region at the origin is not significant.

Under the assumption that $u_0 = 0$, (9) can be integrated to give

$$\frac{g'}{g_0'} = -\alpha^2 + (1 + \alpha^2) \exp\left[-\frac{C_d \pi}{3V}(r^3 - r_0^3) \right]. \tag{12}$$

The maximum extent r_{crit} of the density current can be found by setting $g' = 0$, in which case

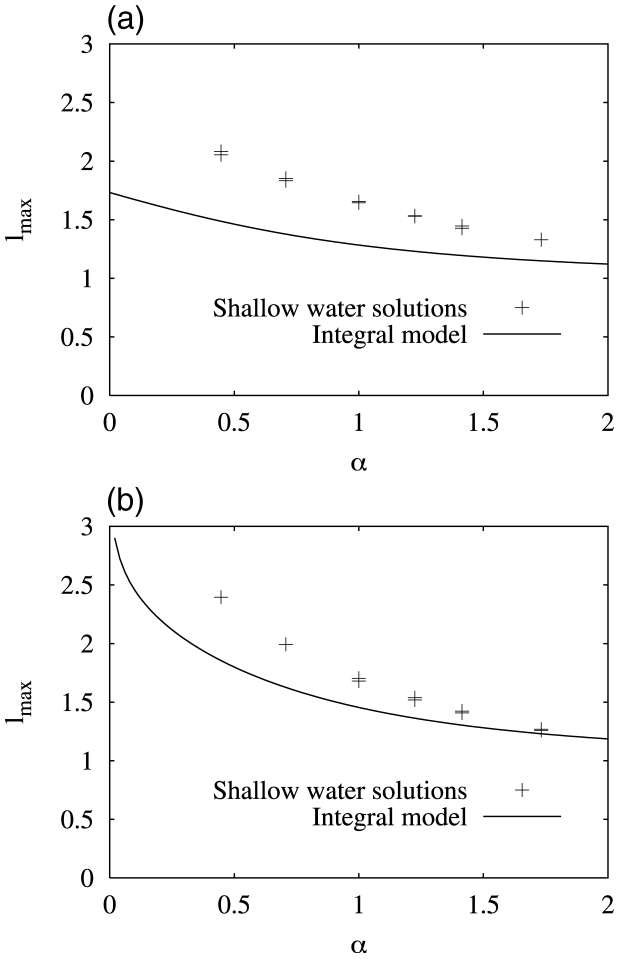

FIG. 6. Runout length of the current as a function of the parameter $\alpha = (-g_s'/g_0')^{1/2}$ for the two cases: (a) $u \ll u_0$ and (b) $u \gg u_0$. The runout length is nondimensionalized with respect to $C_d u_0/V^{3/2} g_0'^{1/2}$. Results from shallow water calculations (with various values of C_d) and the integral model predictions (11) and (13) are shown.

$$r_{\text{crit}} = \left[r_0^3 + \frac{3V}{C_d \pi} \log\left(\frac{1 + \alpha^2}{\alpha^2} \right) \right]^{1/3}. \qquad (13)$$

Note that, in this case, unlike the case with $u \ll u_0$, $r_{\text{crit}} \to \infty$ as $\alpha \to 0$, so it is essential that the surface is colder than the ambient air to ensure the current warms in a finite distance. In practice the speed of the current will fall to a point where u_0 becomes important and this will ensure the heating rate remains high enough to dissipate the current in a finite distance.

In general, even for the case with $\alpha = 0$, (7) and (8) require numerical solutions because of the exponential behavior of (12).

Figure 6b shows a comparison of the runout length from numerical solutions of the shallow water model and the predictions of the integral model as a function of the parameter α, which measures the relative magnitude of the surface heat anomaly and the cold pool anomaly. Again, nondimensionalizing the maximum shallow water distance by $C_d/V^{1/3}$ collapses the data well, showing that the dependence on the aerodynamic drag is the same as for the integral model. The shallow water model also predicts larger maximum radii for the cold pool than the integral model does when $u \gg u_0$, as well as when $u \ll u_0$ and for the same reasons.

6. Atmospheric applications

a. Estimating the spacing of tropical convection

We shall take values from Tompkins (2001b) that we shall assume are typical of tropical convection. Suppose the surface temperature is 300 K, with an atmospheric boundary layer potential temperature of 298 K and an initial cold pool temperature of 297 K. This corresponds to values of 0.05 and -0.10 m s^{-2} for g_0' and g_s', respectively. While it is difficult to estimate the volume of a cold pool, typical formation conditions might be a downdraft of 5 m s^{-1} with a radius of 1.5 km and a density 0.86 times that at the surface. This equates to a volume flux of 3.0×10^7 m^3 s^{-1}. With a typical storm lifetime of 1 h, this gives an initial volume $V = 1.1 \times 10^{11}$ m^3. A realistic value of C_d would be 1.3×10^{-3} in this situation. Using the integral model this gives a maximum extent for the cold pool of 21 km, assuming $u_0 = 7$ m s^{-1}. This is sufficient to assume $u \ll u_0$ as a first approximation. The shallow water model predicts a value approximately 40% larger in this case: approximately 30 km. The time taken for this distance to be reached is approximately 3 h for the shallow water model. This is several times longer than the typical life span of a convective downdraft so the assumption that the cold pool can be treated as an instantaneously released density current is partly justified.

When nondimensionalized, u_0 has a value of approximately 0.45, which is comparable (at least initially) to the speeds in the density current. The assumption that $u_0 \gg u$ is therefore not necessarily true. It is however likely to be a better approximation than assuming $u_0 \ll u$. Including both effects in the shallow water model reduces the predicted maximum extent of the cold pool by about 8% to approximately 27.6 km.

The predicted radius can be compared with the averaged values from a CRM study by Tompkins (2001b), who observed a mean maximum radius of approximately 8.6 km, with a spread of 3–18 km. The mean lifetime of a cold pool was 2.5 h, comparable to the 3 h calculated by the shallow water model. In the CRM, the evolution of a cold pool is more complicated than the simple axisymmetric model described here. Variations in the model mean that the spread of the cold pool is not truly axisymmetric. Triggering of new convection at the front of the cold pool and the collision between two adjacent cold pools can also greatly distort the shape of the cold pool region. The latter effect is particularly relevant since Tompkins (2001b) noted that a majority of convective events triggered at the interface of two

or more mature cold pools. These effects act to reduce the size and lifetime of a typical cold pool. It is perhaps not surprising then that our estimates based on an isolated cold pool are slightly larger than the average values measured by Tompkins in the CRM.

The analytic maximum radius (11) predicted by the integral model in the limit $u \ll u_0$ provides a means of assessing the range of applicability of this model for triggering convection. If $r_{\text{crit}} \approx r_0$, then the warming is so rapid that the density current does not have chance to form and propagate away from the outflow. In this case it is not appropriate to model the cold pool as a density current. This condition is equivalent to

$$\frac{8\text{Fr}V^{3/2}g_0'^{1/2}}{C_d u_0 r_0^4 \pi^{3/2}}\left(1 - \alpha \tan^{-1}\frac{1}{\alpha}\right) \ll 1. \qquad (14)$$

Taking the values for C_d and u_0 given above and assuming the same temperature differences, this would require a current of volume less than 10^{-9} m^3. Alternatively, taking the cold pool size as above and keeping α fixed, the temperature difference between the cold pool and the surrounding air would need to be less than 4×10^{-7} K. A third alternative would be to fix the cold pool volume and temperature, requiring a surface temperature of more than 550 K. None of these conditions are realistic so it would be expected that the surface fluxes will warm the cold pool sufficiently slowly that a density current will form.

The other possibility is that the surface fluxes take so long to act that the current changes very little over a length scale typical for a mesoscale atmospheric phenomenon. In order for r_{crit} to be greater than 100 km, a temperature difference of less than 4×10^{-6} K between the surface and the ambient would be required. In practice other effects, such as entrainment or heat exchange between the cold pool and the ambient, would become important before this limit was reached.

b. *Influence of surface conditions*

It is interesting to consider what influence the surface type would have on this triggering mechanism. The implicit assumption made throughout this work is that the cold pool spreads over a saturated lower boundary, and the previous section compared the simple model to the CRM result of Tompkins (2001b), which were also conducted assuming a tropical ocean lower boundary condition. Replacing this with a land surface has a number of implications. First, it is possible that the relevant value for u_0 in low wind conditions is higher over land surface (Beljaars 1995). Another aspect is that the sensible surface fluxes can be dominated by temperature differences during the day, implying that the approximation $u \ll u_0$ is more relevant, even in low wind scenarios. However, the most complex issue involves the role of water vapor. In the simulations of Tompkins (2001b), the strongly enhanced surface latent heat fluxes played a significant role in maintaining the moisture in the turbulent wake head against the effect of mixing. With a land surface it is possible that the turbulent head moisture could mix out before the cold pool temperature recovers, effectively short-circuiting the mechanism. This emphasizes the requirement for further investigation into the maintenance of the moisture in the cold pool head.

c. *Improving the parameterization of moist convection*

One important goal of this type of research is to improve the representation of these complicated and relatively small-scale processes in larger-scale GCMs. Some progress has already been made in applying the theory of gravity currents to improve the parameterization of the interaction between deep convection and the boundary layer by Qian et al. (1998), who implemented a convective wake parameterization in a single-column version of the National Center for Atmospheric Research (NCAR) Community Climate Model (CCM3). In a study of 12 various observed squall lines, Rozbicki et al. (1999) found that the parameterization resulted in a significant improvement in the correlation between the observed thermodynamic changes across the leading edges of the convective wakes and the thermodynamic characteristics of the modeled downdrafts. While there are differences between the organized squall lines discussed by Rozbicki et al. and the tropical convection discussed here, one could imagine a similar type of parameterization scheme being used. One important difference between the cases is the geometry. With a squall line the wake spreads essentially in a two-dimensional manner out from the squall line, whereas in this case of isolated convection the cold pool spreads radially from the center of the downdraft. The scheme of Rozbicki et al. used the vertical lift at the wake front to feed into the cumulus parameterization scheme and help trigger new convection. The results of Tompkins (2001b) suggest that, for low wind shear cases where the convection is unorganized, it may be the thermodynamical rather than the dynamical properties of the cold pool that control the triggering of new convective cells. One further complication in the case of unorganized convection is the need to account for collisions between cold pools spreading out from nearby downdrafts. Simple models such as that described in this paper may be useful in helping to formulate future convective schemes, possibly based on the work of Qian et al. (1998), to better represent the effects of unorganized convection in global models.

7. Discussion and conclusions

Tompkins (2001b) has presented a convincing argument that the triggering of modeled convective cells in conditions of low winds over the tropical oceans is con-

trolled by thermodynamic rather than dynamical processes in the cold pool. These results are obtained from high-resolution CRM simulations, and there is some limited observational evidence to support the argument. Given the importance of this mechanism in the CRMs, we have shown here how simple models can describe the functional dependence of cold pool behavior (speed, temperature anomaly, runout length). These ideas may be useful in developing new parameterization schemes for moist convection under these types of conditions.

A fundamental requisite for this triggering mechanism is the persistence of a region of high humidity and θ_e near the front of the cold pool. This region is seen in the CRM results, albeit at a limited model resolution. In contrast, simple density current arguments (e.g., Simpson and Britter 1980) lead to continuous and relatively rapid flushing of cold pool air out into the mixed region above (''detraining''). Such processes are not well understood, particularly in the atmosphere where mean state and turbulent profiles are variable. We are left with two extreme models of the cold pool evolution, one in which the fluid properties near the head are persistent and one in which they are rapidly depleted. As yet there is insufficient experimental evidence to resolve between these two extremes. However, there is some laboratory evidence (Lowe et al. 2002) to support the idea of a head region which is only slowly eroded by mixing. Regardless of whether this thermodynamic mechanism is important in the atmosphere, it appears to control the triggering and therefore the statistics of the convection in CRM results. These models are widely used in process studies and in the development of parameterization schemes and are seriously flawed if this mechanism is not in fact physically realistic. It is important that further study is undertaken to establish the applicability of this mechanism: we would argue that such studies need to determine whether persistence of a humid region near the cold pool front is possible.

Acknowledgments. The second author was supported by the Max Planck Institute and a European Union Marie Curie fellowship (FMBICT983005) during this study.

REFERENCES

Beljaars, A. C. M., 1995: The parameterization of surface fluxes in large-scale models under free-convection. *Quart. J. Roy. Meteor. Soc.,* **121,** 255–270.

Benjamin, T. B., 1968: Gravity currents and related phenomena. *J. Fluid Mech.,* **31,** 209–248.

Bonnecaze, R. T., H. E. Huppert, and J. R. Lister, 1993: Particle driven gravity currents. *J. Fluid Mech.,* **250,** 339–369.

——, M. A. Hallworth, H. E. Huppert, and J. R. Lister, 1995: Axisymmetric particle driven gravity currents. *J. Fluid Mech.,* **294,** 93–121.

Britter, R. E., and J. E. Simpson, 1978: Experiments on the dynamics of a gravity current head. *J. Fluid Mech.,* **88** (2), 223–240.

Droegemeier, K. K., and R. B. Wilhelmson, 1987: Numerical simulation of thunderstorm outflow dynamics. Part I: Outflow sensitivity experiments and turbulence dynamics. *J. Atmos. Sci.,* **44,** 1180–1210.

Emanuel, K. A., J. D. Neelin, and C. S. Bretherton, 1994: On large-scale circulations in convecting atmospheres. *Quart. J. Roy. Meteor. Soc.,* **120,** 1111–1143.

Goff, R. C., 1976: Thunderstorm-outflow kinematics and dynamics. NOAA Tech. Memo. ERL NSSL-75, 69 pp.

Grabowski, W. W., 2003: MJO-like coherent structures: Sensitivity simulations using the cloud-resolving convection parameterization (CRCP). *J. Atmos. Sci.,* **60,** 847–864.

Grundy, R. E., and J. W. Rottman, 1985: The approach to self-similarity of the solutions of the shallow-water equations representing gravity current releases. *J. Fluid Mech.,* **156,** 39–53.

Hacker, J., P. F. Linden, and S. B. Dalziel, 1996: Mixing in lock-release gravity currents. *Dyn. Atmos. Oceans,* **24,** 183–195.

Hallworth, M. A., H. E. Huppert, J. C. Phillips, and S. J. Sparks, 1996: Entrainment into two dimensional and axisymmetric turbulent gravity currents. *J. Fluid Mech.,* **308,** 289–311.

Hogg, A. J., H. E. Huppert, and M. A. Hallworth, 1999: Reversing buoyancy of particle-driven gravity currents. *Phys. Fluids,* **11,** 2891–2900.

Hoult, D. P., 1972: Oil spreading on the sea. *Ann. Rev. Fluid Mech.,* **4,** 341–368.

Huppert, H. E., 1998: Quantitative modelling of granular suspension flows. *Philos. Trans. Roy. Soc. London,* **356A,** 2471–2496.

——, and J. E. Simpson, 1980: The slumping of gravity currents. *J. Fluid Mech.,* **99** (4), 785–799.

Jabouille, P., J.-L. Redelsperger, and J. P. Lafore, 1996: Modification of surface fluxes by atmospheric convection in the TOGA COARE region. *Mon. Wea. Rev.,* **124,** 816–837.

Kingsmill, D. E., 1995: Convection initiation associated with a sea-breeze front, a gust front, and their collision. *Mon. Wea. Rev.,* **123,** 2913–2933.

——, and R. A. Houze, 1999: Thermodynamic characteristics of air flowing into and out of precipitating convection over the west Pacific warm pool. *Quart. J. Roy. Meteor. Soc.,* **125,** 1209–1229.

Leonard, B. P., 1988: Simple high accuracy resolution program for convective modelling of discontinuities. *Int. J. Numer. Methods Fluids,* **8,** 1291–1318.

Linden, P. F., and J. E. Simpson, 1986: Gravity-driven flow in a turbulent fluid. *J. Fluid Mech.,* **172,** 481–497.

Liu, C. H., and M. W. Moncrieff, 2000: Simulated density currents in idealized stratified environments. *Mon. Wea. Rev.,* **128,** 1420–1437.

Lowe, R., P. F. Linden, and J. W. Rottman, 2002: A laboratory study of the velocity structure in an intrusive gravity current. *J. Fluid Mech.,* **456,** 33–48.

Moncrieff, M. W., and C. H. Liu, 1999: Convection initiation by density currents: Role of convergence, shear, and dynamical organization. *Mon. Wea. Rev.,* **127,** 2455–2464.

Parker, D. J., 1996: Cold pools in shear. *Quart. J. Roy. Meteor. Soc.,* **122,** 1655–1674.

Press, W. H., S. A. Teukolsky, W. T. Vetterling, and B. P. Flannery, 1992: *Numerical Recipes in C.* 2d ed. Cambridge University Press, 994 pp.

Qian, L., G. S. Young, and W. M. Frank, 1998: A convective wake parameterization scheme for use in general circulation models. *Mon. Wea. Rev.,* **126,** 456–469.

Raymond, D. J., and Z. Zeng, 2000: Instability and large-scale circulations in a two-column model of the tropical troposphere. *Quart. J. Roy. Meteor. Soc.,* **126,** 3117–3135.

Redelsperger, J. L., F. Guichard, and S. Mondon, 2000: A parameterization of mesoscale enhancement of surface fluxes for large-scale models. *J. Climate,* **13,** 402–421.

Reible, D. D., J. E. Simpson, and P. F. Linden, 1993: The sea breeze and gravity-current frontogenesis. *Quart. J. Roy. Meteor. Soc.,* **119,** 1–16.

Rottman, J. W., and J. E. Simpson, 1983: Gravity currents produced by instantaneous releases of a heavy fluid in a rectangular channel. *J. Fluid Mech.,* **135,** 95–110.

Rozbicki, J. J., G. S. Young, and L. Qian, 1999: Test of a convective wake parameterization in the single-column version of CCM3. *Mon. Wea. Rev.*, **127,** 1347–1361.

Simpson, J. E., 1980: Downdrafts as linkages in dynamic cumulus seeding. *J. Appl. Meteor.*, **19,** 477–487.

——, 1997: *Gravity Currents in the Environment and the Laboratory*. 2d ed. Cambridge University Press, 244 pp.

——, and R. E. Britter, 1980: A laboratory model of an atmospheric mesofront. *Quart. J. Roy. Meteor. Soc.*, **106,** 485–500.

Slingo, A., and J. M. Slingo, 1988: The response of a general-circulation model to cloud longwave radiative forcing. 1. Introduction and initial experiments. *Quart. J. Roy. Meteor. Soc.*, **114,** 1027–1062.

Tompkins, A. M., 2001a: On the relationship between tropical convection and sea surface temperature. *J. Climate*, **14,** 633–637.

——, 2001b: Organization of tropical convection in low vertical wind shears: The role of cold pools. *J. Atmos. Sci.*, **58,** 1650–1672.

——, 2001c: Organization of tropical convection in low vertical wind shears: The role of water vapor. *J. Atmos. Sci.*, **58,** 529–545.

Young, G. S., S. M. Perugini, and C. W. Fairall, 1995: Convective wakes in the equatorial western pacific during TOGA. *Mon. Wea. Rev.*, **123,** 110–123.

Zeng, X. B., Q. Zhang, D. Johnson, and W. K. Tao, 2002: Parameterization of wind gustiness for the computation of ocean surface fluxes at different spatial scales. *Mon. Wea. Rev.*, **130,** 2125–2133.